An Analysis of Draw-Wall Wrinkling in a Stamping Die Design

F.-K. Chen and Y.-C. Liao

Department of Mechanical Engineering, National Taiwan University, Taipei, Taiwan

Wrinkling that occurs in the stamping of tapered square cups and stepped rectangular cups is investigated. A common characteristic of these two types of wrinkling is that the wrinkles are found at the draw wall that is relatively unsupported.In the stamping of a tapered square cup, the effect of process parameters, such as the die gap and blank-holder force, on the occurrence of wrinkling is examined using finiteelement simulations. The simulation results show that the larger the die gap, the more severe is the wrinkling, and such wrinkling cannot be suppressed by increasing the blank-holder force. In the analysis of wrinkling that occurred in the stamping of a stepped rectangular cup, an actual production part that has a similar type of geometry was examined. The wrinkles found at the draw wall are attributed to the unbalanced stretching of the sheet metal between the punch head and the step edge. An optimum die design for the purpose of eliminating the wrinkles is determined using finite-element analysis. The good agreement between the simulation results and those observed in the wrinkle-free production part validates the accuracy of the finite-element analysis, and demonstrates the advantage of using finite-element analysis for stamping die design.

Keywords: Draw-wall wrinkle; Stamping die; Stepped rectangular cup; Tapered square cups

1. Introduction

Wrinkling is one of the major defects that occur in the sheet metal forming process. For both functional and visual reasons,wrinkles are usually not acceptable in a finished part. There are three types of wrinkle which frequently occur in the sheet metal forming process: flange wrinkling, wall wrinkling, and elastic buckling of the undeformed area owing to residual elastic compressive stresses. In the forming operation of stamping a complex shape, draw-wall wrinkling means the occurrence of wrinkles in the die cavity. Since the sheet metal in the wall area is relatively unsupported by the tool, the elimination of wall wrinkles is more difficult than the suppression of flange wrinkles. It is well known that additional stretching of the material in the unsupported wall area may prevent wrinkling,and this can be achieved in practice by increasing the blankholder force; but the application of excessive tensile stresses leads to failure by tearing. Hence, the blank-holder force must lie within a narrow range, above that necessary to suppress wrinkles on the one hand, and below that which produces fracture on the other. This narrow range of blank-holder force is difficult to determine. For wrinkles occurring in the central area of a stamped part with a complex shape, a workable range of blank-holder force does not even exist.

In order to examine the mechanics of the formation of wrinkles, Yoshida et al. [1] developed a test in which a thin plate was non-uniformly stretched along one of its diagonals.They also proposed an approximate theoretical model in which the onset of wrinkling is due to elastic buckling resulting from the compressive lateral stresses developed in the non-uniform stress field. Yu et al. [2,3] investigated the wrinkling problem both experimentally and analytically. They found that wrinkling could occur having two circumferential waves according to their theoretical analysis, whereas the experimental results indicated four to six wrinkles. Narayanasamy and Sowerby [4] examined the wrinkling of sheet metal when drawing it through a conical die using flat-bottomed and hemispherical-ended punches. They also attempted to rank the properties that appeared to suppress wrinkling.

These efforts are focused on the wrinkling problems associated with the forming operations of simple shapes only, such as a circular cup. In the early 1990s, the successful application of the 3D dynamic/explicit finite-element method to the sheetmetal forming process made it possible to analyse the wrinkling problem involved in stamping complex shapes. In the present study, the 3D finite-element method was employed to analyse the effects of the process parameters on the metal flow causing wrinkles at the draw wall in the stamping of a tapered square cup, and of a stepped rectangular part.

A tapered square cup, as shown in Fig. 1(*a*), has an inclined draw wall on each side of the cup, similar to that existing in a conical cup. During the stamping process, the sheet metal on the draw wall is relatively unsupported, and is therefore prone to wrinkling. In the present study, the effect of various process parameters on the wrinkling was investigated. In the case of a stepped rectangular part, as shown in Fig. 1(*b*),another type of wrinkling is observed. In order to estimate the effectiveness of the analysis, an actual production part with stepped geometry was examined in the present study. The cause of the wrinkling was determined using finite-element analysis, and an optimum die design was proposed to eliminate the wrinkles. The die design obtained from finite-element analysis was validated by observations on an actual production part.

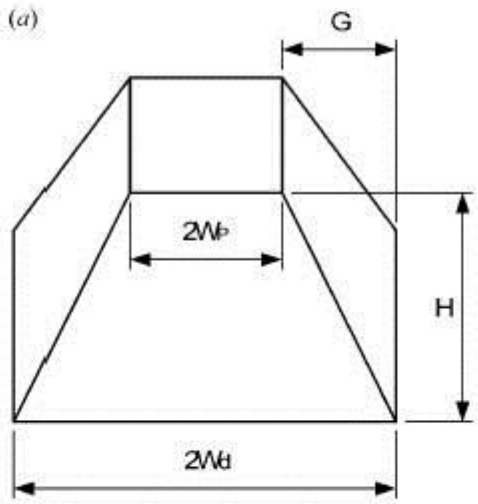

Sketches of (*a*) a tapered square cup.

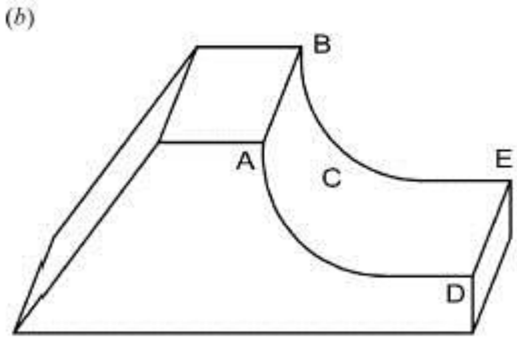

Sketches of(*b*) a stepped rectangular cup.

Fig. 1.

2. Finite-Element Model

The tooling geometry, including the punch, die and blankholder,were designed using the CAD program PRO/ENGINEER. Both the 3-node and 4-node shell elements were adopted to generate the mesh systems for the above tooling using the same CAD program. For the finite-element simulation,the tooling is considered to be rigid, and the corresponding meshes are used only to define the tooling geometry and are not for stress analysis. The same CAD program using 4-node shell elements was employed to construct the mesh system for the sheet blank. Figure 2 shows the mesh system for the complete set of tooling and the sheet-blank used in the stamping of a tapered square cup. Owing to the symmetric conditions, only a quarter of the square cup is analysed. In the simulation, the sheet blank is put on the blank-holder and the die is moved down to clamp the sheet blank against the blank-holder. The punch is then moved up to draw the sheet metal into the die cavity.

In order to perform an accurate finite-element analysis, the actual stress–strain relationship of the sheet metal is required as part of the input data.In the present study, sheet metal with deep-drawing quality is used in the simulations.A tensile test has been conducted for the specimens cut along planes coinciding with the rolling direction (0°) and at angles of 45° and 90° to the rolling direction.The average flow stress σ,calculated from the equation σ=（σ0+2σ45+σ90）/4, for each measured true strain,as shown in Fig.3, is used for the simulations for the stampings of the tapered square cup and also for the stepped rectangular cup.

All the simulations performed in the present study were run on an SGI Indigo 2 workstation using the finite-element program PAMFSTAMP. To complete the set of input data required for the simulations, the punch speed is set to 10 m s_1 and a coefficient of Coulomb friction equal to 0.1 is assumed.

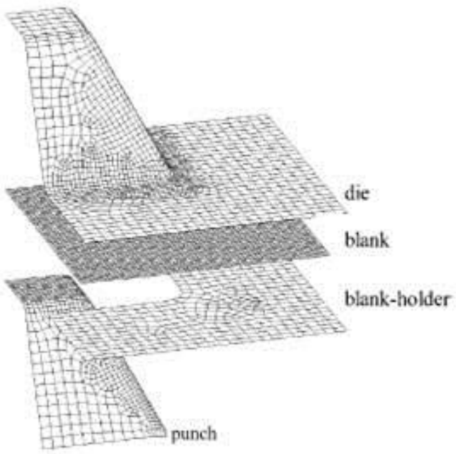

Fig. 2. Finite-element mesh.

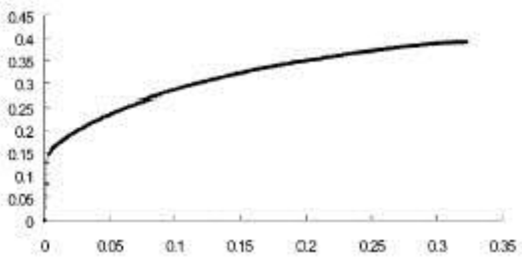

Fig. 3. The stress–strain relationship for the sheet metal.

3. Wrinkling in a Tapered Square Cup

A sketch indicating some relevant dimensions of the tapered square cup is shown in Fig. 1(*a*). As seen in Fig. 1(*a*), the length of each side of the square punch head

(2*Wp*), the die cavity opening (2*Wd*), and the drawing height (*H*) are considered as the crucial dimensions that affect the wrinkling.Half of the difference between the dimensions of the die cavity opening and the punch head is termed the die gap (*G*) in the present study, i.e. $G = Wd\text{-}Wp$. The extent of the relatively unsupported sheet metal at the draw wall is presumably due to the die gap, and the wrinkles are supposed to be suppressed by increasing the blank-holder force. The effects of both the die gap and the blank-holder force in relation to the occurrence of wrinkling in the stamping of a tapered square cup are investigated in the following sections.

3.1 Effect of Die Gap

In order to examine the effect of die gap on the wrinkling, the stamping of a tapered square cup with three different die gaps of 20 mm, 30 mm, and 50 mm was simulated. In each simulation, the die cavity opening is fixed at 200 mm, and the cup is drawn to the same height of 100 mm. The sheet metal used in all three simulations is a 380 mm × 380 mm square sheet with thickness of 0.7 mm, the stress–strain curve for the material is shown in Fig. 3.

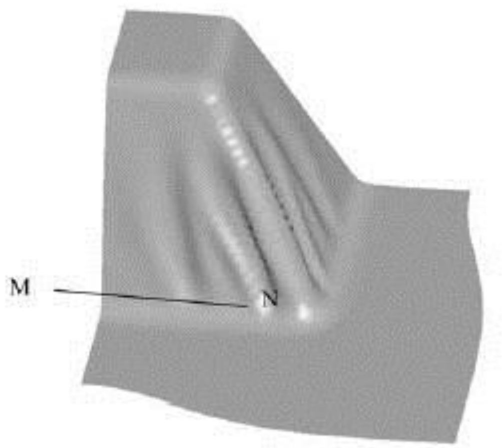

Fig. 4. Wrinkling in a tapered square cup (*G* =50 mm).

The simulation results show that wrinkling occurred in all three tapered square cups, and the simulated shape of the drawn cup for a die gap of 50 mm is shown in Fig. 4. It is seen in Fig. 4 that the wrinkling is distributed on the draw wall and is particularly obvious at the corner between adjacent walls. It is suggested that the wrinkling is due to the large unsupported area at the draw wall during the stamping process,also,the side length of the punch head and the die cavity openingare different owing to the die gap. The sheet metal stretched between the punch head and the die cavity shoulder becomes unstable owing to the presence of compressive transverse stresses. The unconstrained stretching of the sheet metal under compression seems to be the main cause for the wrinkling at the draw wall. In order to compare the results for the three different die gaps, the ratio β of the two principal strains is introduced, β being εmin/εmax, where εmax and εmin are the major and the minor principal strains, respectively. Hosford and Caddell [5] have shown that if the absolute value of β is greater than a critical value, wrinkling is supposed to occur, and the larger the absolute value of β, the greater is the possibility of wrinkling.

The β values along the cross-section *M–N* at the same drawing height for the three simulated shapes with different die gaps, as marked in Fig. 4, are plotted in Fig. 5. It is noted from Fig. 5 that severe wrinkles are located close to the corner and fewer wrinkles occur in the middle of the draw wall for all three different die gaps. It is also noted that the bigger the die gap, the larger is the absolute value of β. Consequently,increasing the die gap will increase the possibility of wrinkling occurring at the draw wall of the tapered square cup.

3.2 Effect of the Blank-Holder Force

It is well known that increasing the blank-holder force can help to eliminate wrinkling in the stamping process. In order to study the effectiveness of increased blank-holder force, the stamping of a tapered square cup with die gap of 50 mm,which is associated with severe wrinkling as stated above, was simulated with different values of blank-holder force. The blank-holder force was increased from 100 kN to 600 kN,which yielded a blank-holder pressure of 0.33 MPa and 1.98 MPa, respectively. The remaining simulation conditions are maintained the same as those specified in the previous section.（An intermediate blank-holder force of 300 kN was also used in the simulation.）

The simulation results show that an increase in the blankholder force does not help to eliminate the wrinkling that occurs at the draw wall.The β values along the cross-section compared with one another for the stamping processes with blank-holder force of 100 kN and 600 kN. The simulation results indicate that the _ values along the cross-section *M–N* are almost identical in both cases. In order to examine the difference of the wrinkle shape for the two different blank-holder forces, five cross-sections of the draw wall at different heights from the bottom to the line *M–N*, as marked in Fig. 4, are plotted in Fig. 6 for both cases.It is noted from Fig. 6 that the waviness of the cross-sections for both cases is similar. This indicates that the blank-holder force does not affect the occurrence of wrinkling in the stamping of a tapered square cup, because the formation of wrinkles is mainly due to the large unsupported area at the draw wall where large compressive transverse stresses exist. The blankholder force has no influence on the instability mode of the material between the punch head and the die cavity shoulder.

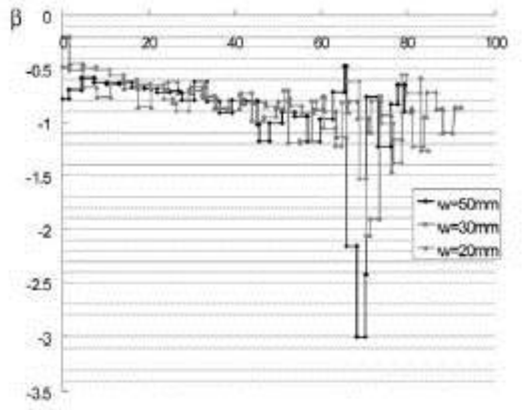

Distance(mm)

Fig. 5. β-value along the cross-section *M–N* for different die gaps.

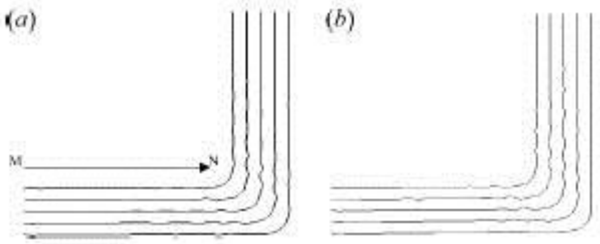

Fig. 6. Cross-section lines at different heights of the draw wall for different blank-holder forces. (*a*) 100 kN. (*b*) 600 kN.

4. Stepped Rectangular Cup

In the stamping of a stepped rectangular cup, wrinkling occurs at the draw wall even though the die gaps are not so significant.Figure 1(*b*) shows a sketch of a punch shape used for stamping a stepped rectangular cup in which the draw wall *C* is followed by a step *D–E*. An actual production part that has this type of geometry was examined in the present study. The material used for this production part was 0.7 mm thick, and the stress–strain relation obtained from tensile tests is shown in Fig. 3.

The procedure in the press shop for the production of this stamping part consists of deep drawing followed by trimming.In the deep drawing process, no draw bead is employed on the die surface to facilitate the metal flow. However, owing to the small punch corner radius and complex geometry, a split occurred at the top edge of the punch and wrinkles were found to occur at the draw wall of the actual production part,as shown in Fig. 7. It is seen from Fig. 7 that wrinkles are distributed on the draw wall, but are more severe at the corner edges of the step, as marked by *A–D* and *B–E* in Fig. 1(*b*).The metal is torn apart along the whole top edge of the punch,as shown in Fig. 7, to form a split.

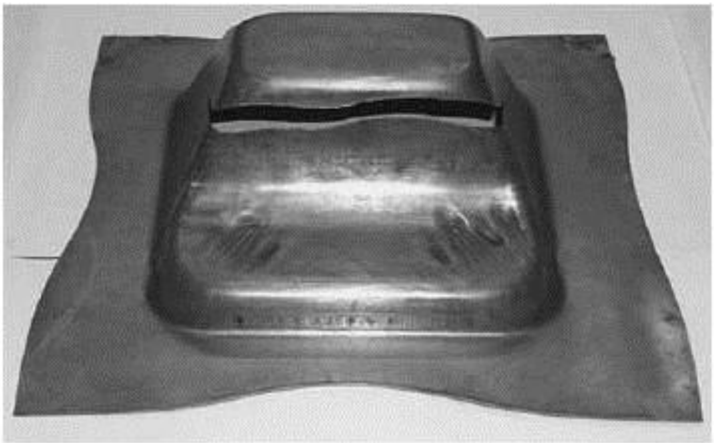

Fig. 7. Split and wrinkles in the production part.

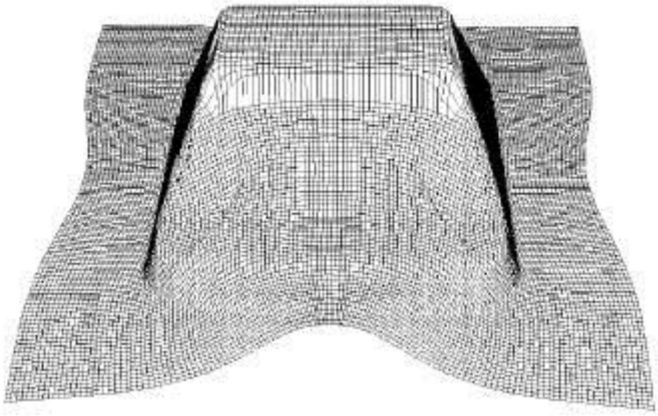

Fig. 8. Simulated shape for the production part with split and wrinkles.

In order to provide a further understanding of the deformation of the sheet-blank during the stamping process, a finiteelement analysis was conducted. The finite-element simulation was first performed for the original design. The simulated shape of the part is shown from Fig. 8. It is noted from Fig.8 that the mesh at the top edge of the part is stretched significantly, and that wrinkles are distributed at the draw wall,similar to those observed in the actual part.The small punch radius, such as the radius along the edge *A*–*B*, and the radius of the punch corner *A*, as marked in Fig.1(*b*), are considered to be the major reasons for the wall breakage. However, according to the results of the finiteelement analysis, splitting can be avoided by increasing the above-mentioned radii. This concept was validated by the actual production part manufactured with larger corner radii.

Several attempts were also made to eliminate the wrinkling.First, the blank-holder force was increased to twice the original value. However, just as for the results obtained in the previous section for the drawing of tapered square cup, the effect of blank-holder force on the elimination of wrinkling was not found to be significant. The same results are also obtained by increasing the friction or increasing the blank size. We conclude that this kind of wrinkling cannot be suppressed by increasing the stretching force.

Since wrinkles are formed because of excessive metal flow in certain regions, where the sheet is subjected to large compressive stresses, a straightforward method of eliminating the wrinkles is to add drawbars in the wrinkled area to absorb the redundant material. The drawbars should be added parallel to the direction of the wrinkles so that the redundant metal can be absorbed effectively. Based on this concept, two drawbars are added to the adjacent walls, as shown in Fig. 9, to absorb the excessive material. The simulation results show that the wrinkles at the corner of the step are absorbed by the drawbars as expected, however some wrinkles still appear at the remaining wall. This indicates the need to put more drawbars at the draw wall to absorb all the excess material. This is, however,not permissible from considerations of the part design.

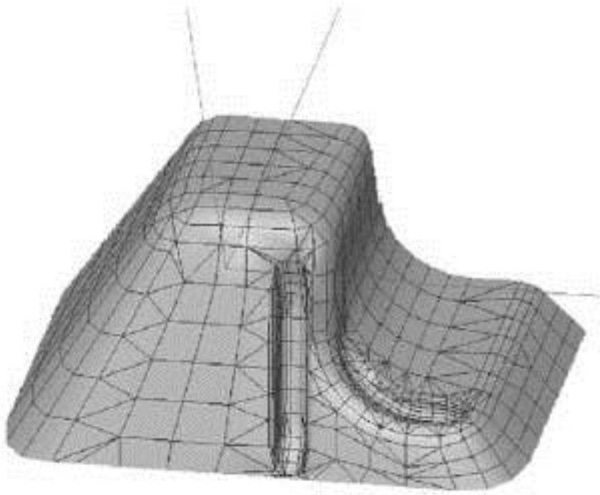

Fig. 9. Drawbars added to the draw walls.

One of the advantages of using finite-element analysis for the stamping process is that the deformed shape of the sheet blank can be monitored throughout the stamping process, which is not possible in the actual production process. A close look at the metal flow during the stamping process reveals that the sheet blank is first drawn into the die cavity by the punch head and the wrinkles are not formed until the sheet blank touches the step edge *D*–*E* marked in Fig. 1(*b*). The wrinkled shape is shown in Fig. 10. This provides valuable information for a possible modification of die design.

Fig. 10. Wrinkle formed when the sheet blank touches the steppededge.

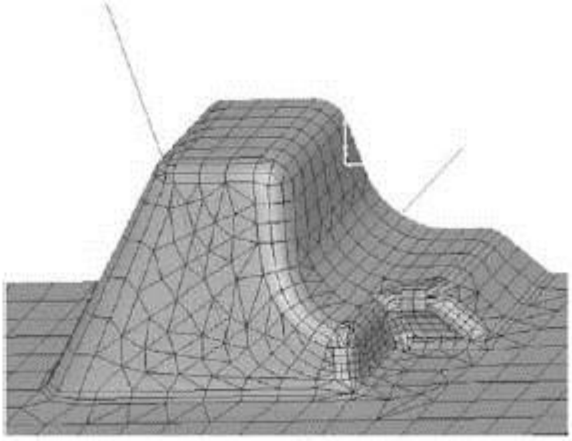

Fig. 11. Cut-off of the stepped corner.

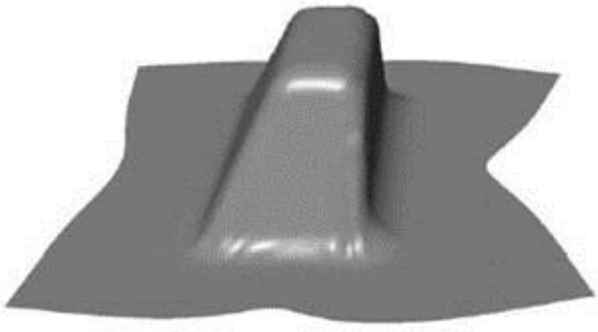

Fig. 12. Simulated shape for the modified die design.

An initial surmise for the cause of the occurrence of wrinkling is the uneven stretch of the sheet metal between the punch corner radius *A* and the step corner radius *D*, as indicated in Fig. 1(*b*). Therefore a modification of die design was carried out in which the step corner was cut off, as shown in Fig.11, so that the stretch condition is changed favourably, which allows more stretch to be applied by increasing the step edges.However, wrinkles were still found at the draw wall of the cup. This result implies that wrinkles are introduced because of the uneven stretch between the whole punch head edge and the whole step edge, not merely between the punch corner and the step corner. In order to verify this idea, two modifications of the die design were suggested: one is to cut the whole step off, and the other is to add one more drawing operation, that is, to draw the desired shape using two drawing operations.The simulated shape for the former method is shown in Fig.12. Since the lower step is cut off, the drawing process is quite similar to that of a rectangular cup drawing, as shown in Fig. 12. It is seen in Fig. 12 that the wrinkles were eliminated.

In the two-operation drawing process, the sheet blank was first drawn to the deeper step, as shown in Fig. 13(*a*). Subsequently,the lower step was formed in the second drawing operation, and the desired shape was then obtained, as shown in Fig. 13(*b*). It is seen clearly in Fig. 13(*b*) that the stepped rectangular cup can be manufactured without wrinkling, by a two-operation drawing process. It should also be noted that in the two-operation drawing process, if an opposite sequence is applied, that is, the lower step is formed first and is followed by the drawing of the deeper step, the edge of the deeper step,as shown by *A*–*B* in Fig. 1(*b*), is prone to tearing because the

metal cannot easily flow over the lower step into the die cavity.

The finite-element simulations have indicated that the die design for stamping the desired stepped rectangular cup using one single draw operation is barely achieved. However, the manufacturing cost is expected to be much higher for the twooperation drawing process owing to the additional die cost and operation cost. In order to maintain a lower manufacturing cost, the part design engineer made suitable shape changes, and modified the die design according to the finite-element

Simulation result to cut off the lower step, as shown in Fig.12. With the modified die design, the actual stamping die for production was manufactured and the production part was found to be free from wrinkles, as shown in Fig.14.The part shape also agreed well with that obtained from the finiteelement simulation.

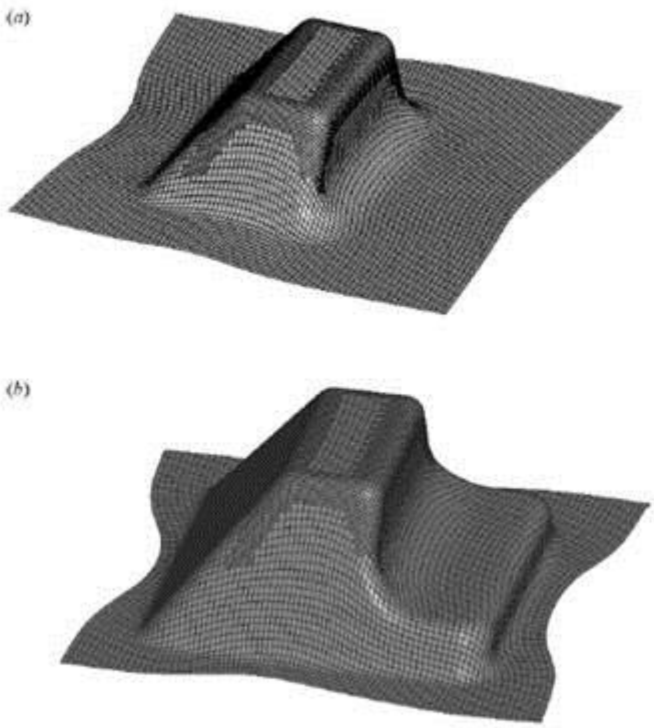

Fig. 13. (*a*) First operation and (*b*) second operation in the two-operation drawing process.

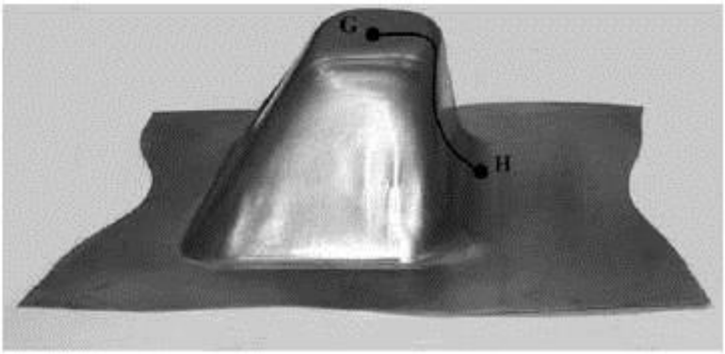

Fig. 14. The defect-free production part.

In order to further validate the finite-element simulation results, the thickness distribution along the cross-section *G–H* obtained from the simulation result as indicated in Fig. 14,was compared with those measured from the production part.The comparison is shown in Fig. 15. It can be seen in Fig.15 that the predicted thickness distribution by finite-element simulation agrees well with that measured directly in the production part. This agreement confirms the effectiveness of the finite-element analysis.

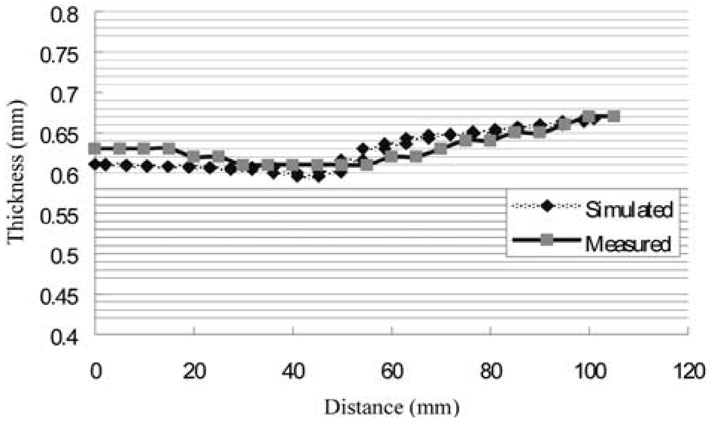

Fig. 15. The simulated and measured thickness distribution along *G–H*.

5. Summary and Concluding Remarks

Two types of wrinkling occurring in stamping processes were investigated using finite-element analysis, and the causes for wrinkling were examined and the methods to eliminate such wrinkles were developed.

The first type of wrinkling appears at the draw wall in the stamping of a tapered square cup. The occurrence of wrinkling is attributed to the large die gap, which is the difference between the side length of the die cavity opening and the side length of the punch head. The large die gap results in a large unsupported area of sheet metal when the metal is drawn into the die cavity and an unfavourable stretch between the punch head and die cavity shoulder. The large unsupported area of sheet metal is therefore prone to wrinkling. The finite-element simulations show that this type of wrinkling cannot be suppressed by increasing the blank-holder force.

Another type of wrinkling investigated occurs in an actual stamping part that has a stepped rectangular geometry. It is found that wrinkling occurs at the draw wall above the step even though the die gap is not sufficiently large. The wrinkling is due to the uneven stretch between the punch head and the step edge, according to the finite-element analysis. Several attempts were made in the die design to eliminate the wrinkling,using finite-element simulations, and an optimum design in which the step was cut off is finally established. The modified die design for eliminating wrinkles was validated by the production of a defect-free production part. The good agreement between the simulation results and those observed in the drawn production part demonstrates the accuracy of the finite-element analysis, and the effectiveness of using finite-element simulations as a substitute for the expensive method of actual die try-outs is thereby confirmed.

Acknowledgements

The authors wish to thank the National Science Council of the Republic of China for the grant NSC-86–2212-E002–028 that made this project possible. They also wish to thank KYM for providing the production part.

References

1. K. Yoshida, H. Hayashi, K. Miyauchi, Y. Yamato, K. Abe, M.Usuda, R. Ishida and Y. Oike, “The effects of mechanical properties of sheet metals on the growth and removing of buckles dueto non-uniform stretching”, Scientific Papers, Institute of Physics and Chemistry Research, 68, pp. 85–93, 1974.
2. T. X. Yu, W. Johnson and W. J. Stronge, “Stamping and springback of circular plates deformed in hemispherical dies”, *International Journal of Mechanical Sciences*, 26, pp. 131–148, 1984.
3. W. J. Stronge, M. P. F. Sutcliffe and T. X. Yu, “Wrinkling of elasto-plastic circular plates during stamping”, Experimental Mechanics, pp. 345–353, 1986.
4. R. Narayanasamy and R. Sowerby, “Wrinkling of sheet metals when drawing through a conical die”, Journal of Material Processing Technology, 41, pp. 275–290, 1994.
5. W. F. Hosford and R. M. Caddell, Metal Forming: Mechanics and Metallurgy, 2nd edn, 1993.

Process simulation in stamping – recent applications for product and process design

W. Thomas*, T. Oenoki and T. Altan

Abstract

Process simulation for product and process design is currently being practiced in industry. However, a number of input variables have a significant effect on the accuracy and reliability of computer predictions. A study was conducted to evaluate the capability of FE-simulations for predicting part characteristics and process conditions in forming complex-shaped, industrial parts.

In industrial applications, there are two objectives for conducting FE-simulations of the stamping process; (1) to optimize the product design by analyzing formability at the product design stage and (2) to reduce the tryout time and cost in process design by predicting the deformation process in advance during the die design stage. For each of these objectives, two kinds of FE-simulations are applied. Pam-Stamp, an

incremental dynamic-explicit FEM code released by Engineering Systems Int'l, matches the second objective well because it can deal with most of the practical stamping parameters. FAST_FORM3D, a one-step FEM code released by Forming Technologies, matches the first objective because it only requires the part geometry and not the complex process information.

In a previous study, these two FE codes were applied to complex-shaped parts used in manufacturing automobiles and construction machinery. Their capabilities in predicting formability issues in stamping were evaluated. This paper reviews the results of this study and summarizes the recommended procedures for obtaining accurate and reliable results from FE simulations.

In another study, the effect of controlling the blank holder force (BHF) during the deep drawing of hemispherical, dome-bottomed cups was investigated. The standard automotive aluminum-killed, drawing-quality (AKDQ) steel was used as well as high performance materials such as high strength steel, bake hard steel, and aluminum 6111. It was determined that varying the BHF as a function of stroke improved the strain distributions in the domed cups.

Author Keywords: Stamping; Process stimulation; Process design

Article Outline

1. Introduction

The design process of complex shaped sheet metal stampings such as automotive panels, consists of many stages of decision making and is a very expensive and time consuming process. Currently in industry, many engineering decisions are made based on the knowledge of experienced personnel and these decisions are typically validated during the soft tooling and prototyping stage and during hard die tryouts. Very often the soft and hard tools must be reworked or even redesigned and remanufactured to provide parts with acceptable levels of quality.

The best case scenario would consist of the process outlined in Fig. 1. In this design process, the experienced product designer would have immediate feedback using a specially design software called one-step FEM to estimate the formability of their design. This would allow the product designer to make necessary changes up front as opposed to down the line after expensive tooling has been manufactured. One-step FEM is particularly suited for product analysis since it does not require binder, addendum, or even most process conditions. Typically this information is not available during the product design phase. One-step FEM is also easy to use and computationally fast, which allows the designer to play “what if” without much time investment.

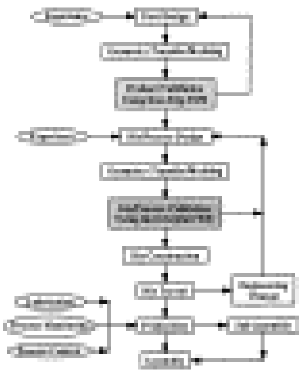

Fig. 1. Proposed design process for sheet metal stampings.

Once the product has been designed and validated, the development project would enter the “time zero” phase and be passed onto the die designer. The die designer would validate his/her design with an incremental FEM code and make necessary design changes and perhaps even optimize the process parameters to ensure not just minimum acceptability of part quality, but maximum achievable quality. This increases product quality but also increase process robustness. Incremental FEM is particularly suited for die design analysis since it does require binder, addendum, and process conditions which are either known during die design or desired to be known.

The validated die design would then be manufactured directly into the hard production tooling and be validated with physical tryouts during which the prototype parts would be made. Tryout time should be decreased due to the earlier numerical validations. Redesign and remanufacturing of the tooling due to unforeseen forming problems should be a thing of the past. The decrease in tryout time and elimination of redesign/remanufacturing should more than make up for the time used to numerically validate the part, die, and process.

Optimization of the stamping process is also of great importance to producers of sheet stampings. By modestly increasing one's investment in presses, equipment, and tooling used in sheet forming, one may increase one's control over the stamping process tremendously. It has been well documented that blank holder force is one of the most sensitive process parameters in sheet forming and therefore can be used to precisely control the deformation process.

By controlling the blank holder force as a function of press stroke AND position around the binder periphery, one can improve the strain distribution of the panel providing increased panel strength and stiffness, reduced springback and residual stresses, increased product quality and process robustness. An inexpensive, but industrial quality system is currently being developed at the ERC/NSM using a combination of hydraulics and nitrogen and is shown in Fig. 2. Using BHF control can also allow engineers to design more aggressive panels to take advantage the increased formability window provided by BHF control.

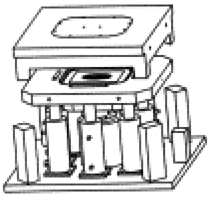

Fig. 2. Blank holder force control system and tooling being developed at the ERC/NSM labs.

Three separate studies were undertaken to study the various stages of the design process. The next section describes a study of the product design phase in which the one-step FEM code FAST_FORM3D (Forming Technologies) was validated with a laboratory and industrial part and used to predict optimal blank shapes. Section 4 summarizes a study of the die design stage in which an actual industrial panel was used to validate the incremental FEM code Pam-Stamp (Engineering Systems Int'l). Section 5 covers a laboratory study of the effect of blank holder force control on the strain distributions in deep drawn, hemispherical, dome-bottomed cups.

2. Product simulation – applications

The objective of this investigation was to validate FAST_FORM3D, to determine FAST_FORM3D's blank shape prediction capability, and to determine how one-step FEM can be implemented into the product design process. Forming Technologies has provided their one-step FEM code FAST_FORM3D and training to the ERC/NSM for the purpose of benchmarking and research. FAST_FORM3D does not simulate the deformation history. Instead it projects the final part geometry onto a flat plane or developable surface and repositions the nodes and elements until a minimum energy state is reached. This process is computationally faster than incremental simulations like Pam-Stamp, but also makes more assumptions.

FAST_FORM3D can evaluate formability and estimate optimal blank geometries and is a strong tool for product designers due to its speed and ease of use particularly during the stage when the die geometry is not available.

In order to validate FAST_FORM3D, we compared its blank shape prediction with analytical blank shape prediction methods. The part geometry used was a 5 in. deep 12 in. by 15 in. rectangular pan with a 1 in. flange as shown in Fig. 3. Table 1 lists the process conditions used. Romanovski's empirical blank shape method and the slip line field method was used to predict blank shapes for this part which are shown in Fig. 4.

Fig. 3. Rectangular pan geometry used for FAST_FORM3D validation.

Table 1. Process parameters used for FAST_FORM3D rectangular pan validation

Mechanical properties of material		
Young's Modulus	E	200 Gpa
Poisson's Ratio	ν	0.3
Yield stress	σ_y	179.0 MPa
Flow stress curve	K	536.5 MPa
$[\sigma=K(\varepsilon+\varepsilon_0)^n]$	n	0.227
	ε_0	0.0044
Normal anisotropy	r_0	1.80
	r_{45}	1.29
	r_{90}	2.10
Thickness	t	0.84 mm
Process parameters		
Friction coefficient	μ	0.10
Blank hold pressure	p	0.60 MPa

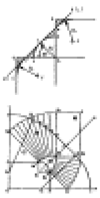

Fig. 4. Blank shape design for rectangular pans using hand calculations. (a) Romanovski's empirical method; (b) slip line field analytical method.

Fig. 5(a) shows the predicted blank geometries from the Romanovski method, slip line field method, and FAST_FORM3D. The blank shapes agree in the corner area, but differ greatly in the side regions. Fig. 5(b)–(c) show the draw-in pattern after the drawing process of the rectangular pan as simulated by Pam-Stamp for each of the predicted blank shapes. The draw-in patterns for all three rectangular pans matched in the corners regions quite well. The slip line field method, though, did not achieve the objective 1 in. flange in the side region, while the Romanovski and FAST_FORM3D methods achieved the 1 in. flange in the side regions relatively well. Further, only the FAST_FORM3D blank agrees in the corner/side transition regions. Moreover, the FAST_FORM3D blank has a better strain distribution and lower peak strain than Romanovski as can be seen in Fig. 6.

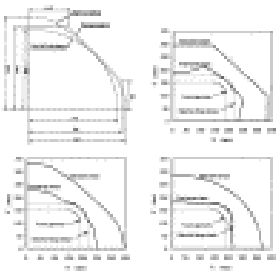

Fig. 5. Various blank shape predictions and Pam-Stamp simulation results for the rectangular pan. (a) Three predicted blank shapes; (b) deformed slip line field blank; (c) deformed Romanovski blank; (d) deformed FAST_FORM3D blank.

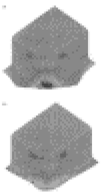

Fig. 6. Comparison of strain distribution of various blank shapes using Pam-Stamp for the rectangular pan. (a) Deformed Romanovski blank; (b) deformed FAST_FORM3D blank.

To continue this validation study, an industrial part from the Komatsu Ltd. was chosen and is shown in Fig. 7(a). We predicted an optimal blank geometry with FAST_FORM3D and compared it with the experimentally developed blank shape as shown in Fig. 7(b). As seen, the blanks are similar but have some differences.

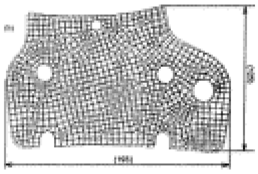

Fig. 7. FAST_FORM3D simulation results for instrument cover validation. (a) FAST_FORM3D's formability evaluation; (b) comparison of predicted and experimental blank geometries.

Next we simulated the stamping of the FAST_FORM3D blank and the experimental blank using Pam-Stamp. We compared both predicted geometries to the nominal CAD geometry (Fig. 8) and found that the FAST_FORM3D geometry was much more accurate. A nice feature of FAST_FORM3D is that it can show a “failure” contour plot of the part with respect to a failure limit curve which is shown in Fig. 7(a). In conclusion, FAST_FORM3D was successful at predicting optimal blank shapes for a laboratory and industrial parts. This indicates that FAST_FORM3D can be successfully used to assess formability issues of product designs. In the case of the instrument cover, many hours of trial and error experimentation could have been eliminated by using FAST_FORM3D and a better blank shape could have been developed.

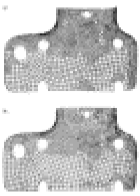

Fig. 8.
Comparison of FAST_FORM3D and experimental blank shapes for the instrument cover. (a) Experimentally developed blank shape and the nominal CAD geometry; (b) FAST_FORM3D optimal blank shape and the nominal CAD geometry.

3. Die and process simulation – applications

In order to study the die design process closely, a cooperative study was conducted by Komatsu Ltd. of Japan and the ERC/NSM. A production panel with forming problems was chosen by Komatsu. This panel was the excavator's cabin, left-hand inner panel shown in Fig. 9. The geometry was simplified into an experimental laboratory die, while maintaining the main features of the panel. Experiments were conducted at Komatsu using the process conditions shown in Table 2. A forming limit diagram (FLD) was developed for the drawing-quality steel using dome tests and a vision strain measurement system and is shown in Fig. 10. Three blank holder forces (10, 30, and 50 ton) were used in the experiments to determine its effect. Incremental simulations of each experimental condition was conducted at the ERC/NSM using Pam-Stamp.

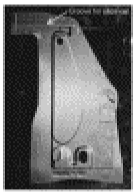

Fig. 9. Actual product – cabin inner panel.

Table 2. Process conditions for the cabin inner investigation

Part depth: 50 mm
Material: SPCE (JIS standard)
Blank: 785 mm by 815 mm
Thickness: 1.6 mm
BHF: 10, 30, 50 ton
Coefficient of friction (μ): 0.6/0.10
Flow stress: σ=0.5693(0.0072+$\varepsilon^{0.247}$) GPa
Normal anisotropy: 2.21
Punch velocity: 5 mm/ms
Mesh: 12 mm (3 or 6 mm after refinement)
FLD determined with Ø50 mm hemispherical dome tests and 3 mm circle grids. Strains measured with a 3-D vision system by CamSys Inc.

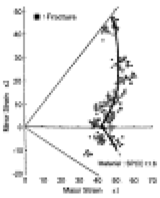

Fig. 10. Forming limit diagram for the drawing-quality steel used in the cabin inner investigation.

At 10 ton, wrinkling occurred in the experimental parts as shown in Fig. 11. At 30 ton, the wrinkling was eliminated as shown in Fig. 12. These experimental observations were predicted with Pam-stamp simulations as shown in Fig. 13. The 30 ton panel was measured to determine the material draw-in pattern. These measurements are compared with the predicted material draw-in in Fig. 14. Agreement was very good, with a maximum error of only 10 mm. A slight neck was observed in the 30 ton panel as shown in Fig. 13. At 50 ton, an obvious fracture occurred in the panel.

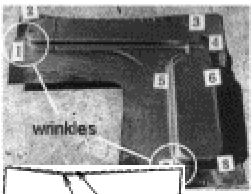

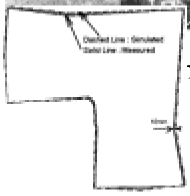

ıg in laboratory cabin inner panel, BHF=10 ton.

Fig. 12. Deformation stages of the laboratory cabin inner and necking, BHF=30 ton. (a) Experimental blank; (b) experimental panel, 60% formed; (c) experimental panel, fully formed; (d) experimental panel, necking detail.

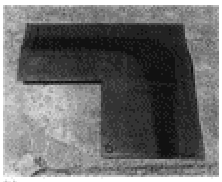

(a)

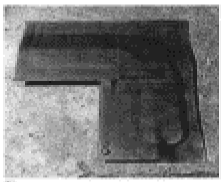

(b)

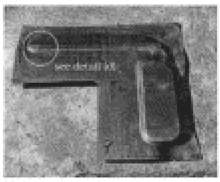

(c)

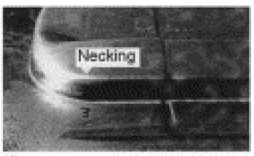

(d)

Fig. 13. Predication and elimination of wrinkling in the laboratory cabin inner. (a) Predicted geometry, BHF=10 ton; (b) predicted geometry, BHF=30 ton.

Fig. 14. Comparison of predicted and measured material draw-in for lab cabin inner, BHF=30 ton.

Strains were measured with the vision strain measurement system for each panel, and the results are shown in Fig. 15. The predicted strains from FEM simulations for each panel are shown in Fig. 16. The predictions and measurements agree well regarding the strain distributions, but differ slightly on the effect of BHF. Although the trends are represented, the BHF tends to effect the strains in a more localized manner in the simulations when compared to the measurements. Nevertheless, these strain prediction show that Pam-Stamp correctly predicted the necking and fracture which occurs at 30 and 50 ton. The effect of friction on strain distribution was also investigated with simulations and is shown in Fig. 17.

Fig. 15. Experimental strain measurements for the laboratory cabin inner. (a) measured strain, BHF=10 ton (panel wrinkled); (b) measured strain, BHF=30 ton (panel necked); (c) measured strain, BHF =50 ton (panel fractured).

Fig. 16. FEM strain predictions for the laboratory cabin inner. (a) Predicted strain, BHF=10 ton; (b) predicted strain, BHF=30 ton; (c) predicted strain, BHF=50 ton.

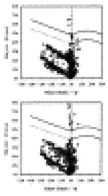

Fig. 17. Predicted effect of friction for the laboratory cabin inner, BHF=30 ton. (a) Predicted strain, μ=0.06; (b) predicted strain, μ=0.10.

A summary of the results of the comparisons is included in Table 3. This table shows that the simulations predicted the experimental observations at least as well as the strain measurement system at each of the experimental conditions. This indicates that Pam-Stamp can be used to assess formability issues associated with the die design.

Table 3. Summary results of cabin inner study

BHF (ton)	Experimental observations	Simulated predictions
10	Wrinkling	Wrinkling
30	Necking	Necking/fracture
50	Fracture	Necking/fracture

4. Blank holder force control – applications

The objective of this investigation was to determine the drawability of various, high performance materials using a hemispherical, dome-bottomed, deep drawn cup (see Fig. 18) and to investigate various time variable blank holder force profiles. The materials that were investigated included AKDQ steel, high strength steel, bake hard steel, and aluminum 6111 (see Table 4). Tensile tests were performed on these materials to determine flow stress and anisotropy characteristics for analysis and for input into the simulations (see Fig. 19 and Table 5).

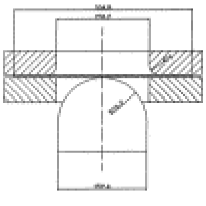

Fig. 18. Dome cup tooling geometry.

Table 4. Material used for the dome cup study

Material	Thickness (mm)	Diameter (mm)
AKDQ steel	0.81	304.8
Aluminum 6111	1.20	304.8
High-strength steel	0.86	304.8

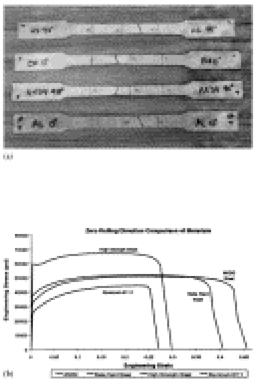

Fig. 19. Results of tensile tests of aluminum 6111, AKDQ, high strength, and bake hard steels. (a) Fractured tensile specimens; (b) Stress/strain curves.

Table 5. Tensile test data for aluminum 6111, AKDQ, high strength, and bake hard steels

	E (psi)	K (psi)	n	r
AKDQ steel (0.032 in.)				
0°	2.47E+07	81945	0.203	1.059
45°	2.52E+07	82658	0.184	1.484
90°	2.25E+07	80506	0.205	1.419
Average	2.44E+07	81942	0.194	1.361
Range	−1.54E+06	−1433	0.020	−0.245
High strength steel (0.034 in.)				
0°	2.13E+07	100 121	0.138	–
45°	2.48E+07	91817	0.151	–
90°	2.40E+07	100 941	0.150	–
Average	2.37E+07	96174	0.147	–
Range	−2.18E+06	8714	−0.007	–
Aluminum 6111 (0.040 in.)				
0°	9.34E+06	80855	0.248	0.680
45°	9.27E+06	77491	0.250	0.594
90°	9.38E+06	77746	0.253	0.541
Average	9.32E+06	78396	0.250	0.602
Range	8.59E+04	1809	0.001	0.017
Bake hard steel (0.032 in.)				
0°	2.34E+07	82837	0.171	1.264
45°	2.64E+07	82138	0.159	0.551
90°	2.81E+07	78897	0.151	1.116
Average	2.61E+07	81502	0.160	0.871
Range	−6.08E+05	−1270	0.002	0.639

It is interesting to note that the flow stress curves for bake hard steel and AKDQ steel were very similar except for a 5% reduction in elongation for bake hard. Although, the elongations for high strength steel and aluminum 6111 were similar, the n-value for aluminum 6111 was twice as large. Also, the r-value for AKDQ was much bigger than 1, while bake hard was nearly 1, and aluminum 6111 was much less than 1.

The time variable BHF profiles used in this investigation included constant, linearly decreasing, and pulsating (see Fig. 20). The experimental conditions for AKDQ steel were simulated using the incremental code Pam-Stamp. Examples of wrinkled, fractured, and good laboratory cups are shown in Fig. 21 as well as an image of a simulated wrinkled cup.

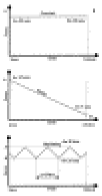

Fig. 20. BHF time-profiles used for the dome cup study. (a) Constant BHF; (b) ramp BHF; (c) pulsating BHF.

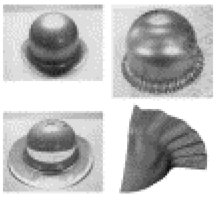

Fig. 21. Experimental and simulated dome cups. (a) Experimental good cup; (b) experimental fractured cup; (c) experimental wrinkled cup; (d) simulated wrinkled cup.

Limits of drawability were experimentally investigated using constant BHF. The results of this study are shown in Table 6. This table indicates that AKDQ had the largest drawability window while aluminum had the smallest and bake hard and high strength steels were in the middle. The strain distributions for constant, ramp, and pulsating BHF are compared experimentally in Fig. 22 and are compared with simulations in Fig. 23 for AKDQ. In both simulations and experiments, it was found that the ramp BHF trajectory improved the strain distribution the best. Not only were peak strains reduced by up to 5% thereby reducing the possibility of fracture, but low strain regions were increased. This improvement in strain distribution can increase product stiffness and strength, decrease springback and residual stresses, increase product quality and process robustness.

Table 6. Limits of drawability for dome cup with constant BHF

	Wrinkling limit (ton)	Best (ton)	Fracture limit (ton)
Aluminum	6	7	9
AKDQ	6	20	35
High strength steel	7	15	25

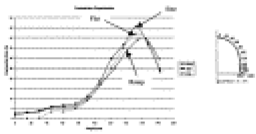

Fig. 22. Experimental effect of time variable BHF on engineering strain in an AKDQ steel dome cup.

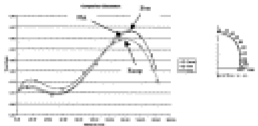

Fig. 23. Simulated effect of time variable BHF on true strain in an AKDQ steel dome cup.

Pulsating BHF, at the frequency range investigated, was not found to have an effect on strain distribution. This was likely due to the fact the frequency of pulsation that was tested was only 1 Hz. It is known from previous experiments of other researchers that proper frequencies range from 5 to 25 Hz [3]. A comparison of load-stroke curves from simulation and experiments are shown in Fig. 24 for AKDQ. Good agreement was found for the case where μ=0.08. This indicates that FEM simulations can be used to assess the formability improvements that can be obtained by using BHF control techniques.

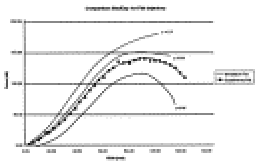

Fig. 24. Comparison of experimental and simulated load-stroke curves for an AKDQ steel dome cup.

5. Conclusions and future work

In this paper, we evaluated an improved design process for complex stampings which involved eliminating the soft tooling phase and incorporated the validation of product and process using one-step and incremental FEM simulations. Also, process improvements were proposed consisting of the implementation of blank holder force control to increase product quality and process robustness.

Three separate investigations were summarized which analyzed various stages in the design process. First, the product design phase was investigated with a laboratory and industrial validation of the one-step FEM code FAST_FORM3D and its ability to assess formability issues involved in product design. FAST_FORM3D was successful at predicting optimal blank shapes for a rectangular pan and an industrial instrument cover. In the case of the instrument cover, many hours of trial and error experimentation could have been eliminated by using FAST_FORM3D and a better blank shape could have been developed.

Second, the die design phase was investigated with a laboratory and industrial validation of the incremental code Pam-Stamp and its ability to assess forming issues associated with die design. This investigation suggested that Pam-Stamp could predict strain distribution, wrinkling, necking, and fracture at least as well as a vision strain measurement system at a variety of experimental conditions.

Lastly, the process design stage was investigated with a laboratory study of the quality improvements that can be realized with the implementation of blank holder force control techniques. In this investigation, peak strains in hemispherical, dome-bottomed, deep drawn cups were reduced by up to 5% thereby reducing the possibility of fracture, and low strain regions were increased. This improvement in strain distribution can increase product stiffness and strength, decrease springback and residual stresses, increase product quality and process robustness. It can be expected that improvements in drawability would be further enhanced by optimizing the variation of the BHF in function of time. Further, good agreement was found for experimentally measured and numerically predicted load-stroke curves indicating that FEM simulations can be used to assess the formability improvements that can be obtained using BHF control techniques.